Jurnal Teknik Informatika (JUTIF)
P-ISSN: 2723-3863
E-ISSN: 2723-3871
Vol. 6, No. 4, Agustus 2025, Page. 2035-2052
https://jutif.if.unsoed.ac.id
DOI: https://doi.org/10.52436/1.jutif.6.4.4880

Palm Oil Seed Origin Classification Based on Thermal Images and Agricultural Data Using Convolutional Neural Network

Si Gede Ngurah Chandra Adi Natha*[1], Tjokorda Agung Budi Wirayuda[2], Rifki Wijaya[3]

[1,2,3]Department Of Informatics, Telkom University Bandung, Indonesia

Email: [1]ngurahchandraa@student.telkomuniversity.ac.id

Received : Jun 13, 2025; Revised : Jul 15, 2025; Accepted : Jul 20, 2025; Published : Aug 18, 2025

Abstract

The traceability of palm oil seed origins plays a vital role in ensuring transparency, legality, and sustainability across the palm oil supply chain. Recent advances in deep learning have created new opportunities to improve classification systems by leveraging both visual and contextual data. This study proposes a deep learning-based model for classifying the origin of palm oil seeds by integrating thermal imagery with agricultural data. Two convolutional neural network (CNN) architectures, ResNet50 and MobileNet, were evaluated under three experimental setups: using only thermal images, combining thermal images with agricultural features (socio-economic, soil, and spectral fruit characteristics), and applying hyperparameter tuning to the best-performing model. The results show that ResNet50 consistently outperformed MobileNet, particularly in multimodal configurations. The highest performance was achieved using ResNet50 with the Adam optimizer, a learning rate of 0.001, and a batch size of 16, resulting in training accuracy of 99.75%, validation accuracy of 99.92%, and test accuracy of 100.00%. Evaluation metrics confirmed the model's robustness with precision, recall, and F1-score all reaching 100.00%. This research highlights the significant potential of combining thermal imagery and agricultural data in CNN-based models for accurate and reliable classification of palm oil seed origins. The approach can support traceability systems in the palm oil industry, offering a scalable and data-driven solution for ensuring supply chain integrity and sustainability.

Keywords : *Agricultural Data, Convolutional Neural Network, Multimodal Deep Learning, Palm Oil Seed Origin, Thermal Image Classification.*

1. INTRODUCTION

Palm oil is one of the most significant agricultural commodities globally, contributing greatly to various industries such as food, cosmetics, and bioenergy [1]. The palm oil industry in Indonesia, in particular, plays an important role in the global economy. According to data from the Central Statistics Agency (BPS), in 2023, Indonesia had approximately 15.93 million hectares of oil palm plantations with a total production of 47.08 million tons. In terms of exports, "Other Palm Oil" accounted for 81.83% of total exports, followed by Crude Palm Oil (CPO) at 13.06%, Other Palm Kernel Oil at 4.97%, and Crude Palm Kernel Oil at 0.14%. This data demonstrates Indonesia's dominance as a global producer and exporter of palm oil [2].

With the increasing demand for sustainable agricultural products that have traceable origins, identifying the provenance of palm oil seeds has become a crucial aspect in the palm oil supply chain [3], [4], [5]. Accurate traceability ensures products come from legal and eco-friendly sources, while supporting audits, certifications, and regulatory compliance [6]. A reliable classification system for seed origin can enhance transparency and build trust among consumers and stakeholders [7], [8].

Conventional methods of determining the origin of palm oil seeds generally still rely on manual records, laboratory testing, or supply chain documentation, that are labor-intensive, expensive, and

Vol. 6, No. 4, Agustus 2025, Page. 2035-2052
https://jutif.if.unsoed.ac.id
DOI: https://doi.org/10.52436/1.jutif.6.4.4880

susceptible to mistakes [9], [10]. Therefore, more efficient and automated solutions are needed, one of which is by combining image processing and machine learning techniques [11], [12], [13].

To date, thermal imaging has been widely applied in agricultural settings, particularly in assessing fruit maturity and plant stress [14], [15], [16], [17]. However, its specific application for classifying the origin of palm oil seeds remains limited, offering an opportunity for further exploration in this study. In particular, supporting agricultural data such as soil type, spectral fruit data, and socio-economic variables can enhance classification accuracy and enable more reliable identification of seed origin [18].

Convolutional Neural Networks (CNN) have proven highly effective in image classification tasks, including agricultural applications. One widely used CNN architecture is ResNet50, which employs residual connections to mitigate vanishing gradient problems in deep networks [19], [20]. This enables training of very deep models with improved feature extraction, making ResNet50 suitable for complex image data such as thermal images of palm oil seeds. Another architecture is MobileNet, designed to be lightweight and efficient by using depthwise separable convolutions [21], [22]. This design allows MobileNet to be deployed on resource-constrained devices without significant loss in accuracy.

Previous research showed that the ResNet50 model can classify the fresh fruit bunches (FFB) maturity of oil palm into two classes with 97% accuracy [23]. The model achieved strong results in precision, recall, and F1-score using an optimal setup consisting of a 90:10 data split, the Adam optimizer, and a 0.0001 learning rate. Meanwhile, a study developed an adapted and optimized MobileNet model to detect and classify strawberries and cherries in outdoor environments [24]. By modifying the original MobileNet architecture, like substituting the upper layers and eliminating the fully connected layer, the model attained an average validation accuracy of 98.60% with a loss percentage of merely 0.38%, indicating elevated classification accuracy with minimal computational expense. Additionally, another research demonstrated that concatenating features extracted from multiple models can improve tomato leaf disease classification accuracy, achieving a best accuracy of 97% [25].

Building upon these considerations, this research investigates the effectiveness of two different CNN architectures, ResNet50 and MobileNet, in classifying the origin of palm oil seeds based on thermal images and agricultural data. The research is conducted in three stages: (1) classification using thermal images only, (2) combined classification with agricultural data, and (3) hyperparameter tuning regarding the highest-performing model. The results of this research aim to aid in developing a more accurate, dependable, and data-driven system for identifying the origins of palm oil seeds.

2. METHOD

The overall workflow of the palm oil seed origin classification process is illustrated in Figure 1. The system comprises several stages, beginning with data acquisition involving thermal imagery and the collection of agricultural data, such as socio-economic, soil, and fruit spectral characteristics. This is followed by a data preparation phase that includes handling missing values, selecting relevant features, applying normalization techniques, and splitting the dataset into training, validation, and testing sets. The prepared data is then used to train two convolutional neural network (CNN) architectures, ResNet50 and MobileNet, under two input scenarios: one using only thermal images and another combining thermal images with agricultural data. The best-performing model is further optimized through hyperparameter tuning to improve accuracy and robustness. This step-by-step process is summarized as shown in Figure 1.

Jurnal Teknik Informatika (JUTIF)
P-ISSN: 2723-3863
E-ISSN: 2723-3871
Vol. 6, No. 4, Agustus 2025, Page. 2035-2052
https://jutif.if.unsoed.ac.id
DOI: https://doi.org/10.52436/1.jutif.6.4.4880

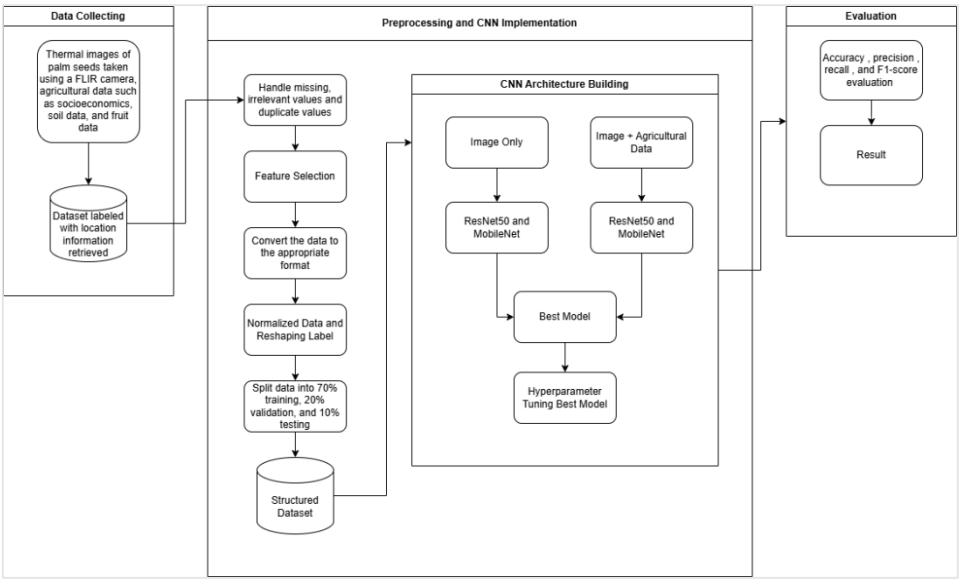

Figure 1. Palm Oil Seed Origin Classification Workflow

2.1. Dataset

The dataset utilized in this study is part of a research project conducted by the Research Center for Rural Development and Sustainable Agriculture at Syiah Kuala University. It consists of a total of 7,257 thermal images of palm oil seeds, categorized into 73 distinct class labels representing different seed origins. Alongside the thermal images, supporting agricultural data is collected, including soil properties, spectral fruit data, and socio-economic variables. These agricultural data are numerical and labeled according to the same class scheme.

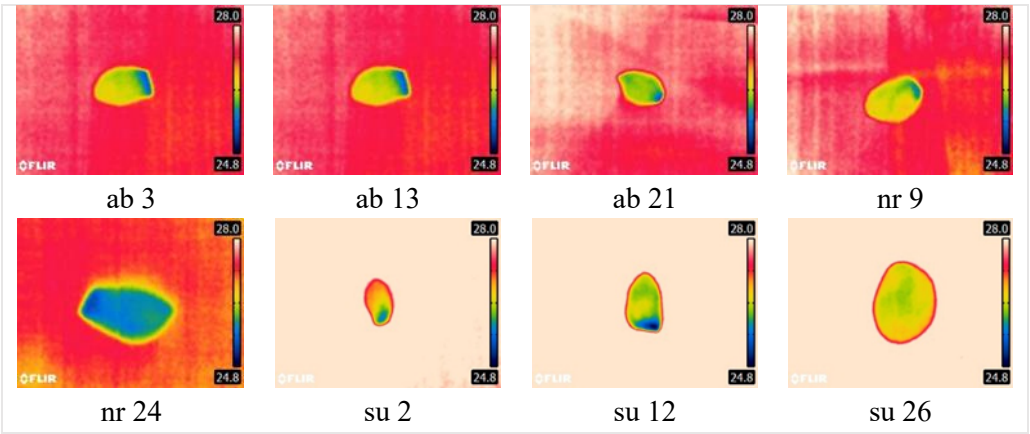

Figure 2. Thermal Image of Palm Oil Seeds Sample

Figure 2 illustrates a selection of sample thermal images from the dataset. Each image corresponds to a specific palm oil seed origin and is captured using a thermal imaging device. The figure highlights the visual differences in thermal signatures across seed origins, which are later used as input to the CNN model. This visual representation provides insight into the nature of thermal variations present in the dataset.

Table 1 presents example entries of the class labeling scheme used in this study. It includes information such as the class name, the actual location name, and the sample location where the seed was collected. The table helps contextualize the diversity and distribution of the seed origins, providing

Vol. 6, No. 4, Agustus 2025, Page. 2035-2052
https://jutif.if.unsoed.ac.id
DOI: https://doi.org/10.52436/1.jutif.6.4.4880

an overview of the spatial labeling used for both the thermal and agricultural data. Only 8 out of the 73 class labels are shown for illustration purposes.

Table 1. Corresponding Class Name and Descriptions

Class name	Location name	Sample location
ab 3	Aceh Barat Daya	3
ab 13	Aceh Barat Daya	13
ab 21	Aceh Barat Daya	21
nr 9	Nagan Raya	9
nr 24	Nagan Raya	24
su 2	Subulussalam	2
su 12	Subulussalam	12
su 26	Subulussalam	26

2.2. Pre-processing Data

Data preprocessing is a vital and crucial stage in preparing the dataset to ensure it is clean, consistent, and suitable for model training [26]. This process addresses common data quality issues involving missing values, duplications, and inconsistency, as well as transforming and normalizing data to meet the requirements of the CNN architectures [27]. In this study, several preprocessing steps were carried out on both thermal images and supporting agricultural data. Thermal images were normalized and resized to a consistent resolution compatible with the CNN input requirements. Meanwhile, agricultural data including soil properties, spectral fruit data, and socio-economic variables underwent cleaning, normalization, and encoding to convert categorical variables into numerical formats.

2.2.1. Handling Missing, Irrelevant and Duplicates Data in Agriculture Data

This step focuses on preparing and refining the agricultural dataset to ensure its preparedness for later examination and modeling. Initially, the dataset is examined to identify which features are relevant and suitable for use. Irrelevant or unnecessary data are removed to streamline the dataset, and the cleaned data are saved for further processing [28]. In cases where duplicate entries are detected, these records are consolidated by averaging their values according to their class labels. Furthermore, missing data points are addressed by imputing the average value associated with that specific feature, thereby preserving the dataset's completeness and reliability [29]. This process ensures that the final dataset contains only pertinent features that contribute effectively to model training while maintaining high data quality.

2.2.2. Feature Selection for Agriculture Data

Feature selection is utilized to determine the most significant and relevant features associated with the target labels, while excluding those that are less informative or redundant [30]. This process aims to enhance model performance and computational efficiency by reducing the data's dimensionality, accelerating training time, and minimizing overfitting risk. By focusing on the most predictive attributes in the dataset, the model's generalization capability is improved. In this study, Correlation-based Feature Selection (CFS) utilizing Pearson Correlation is applied as the feature selection method. This technique assesses how each feature is linearly associated with the target variable to determine relevance, while simultaneously examining inter-feature correlations to detect redundancy [31]. Consequently, CFS yields an optimized subset of features that are both highly relevant to the target and minimally redundant,

Vol. 6, No. 4, Agustus 2025, Page. 2035-2052
https://jutif.if.unsoed.ac.id
DOI: https://doi.org/10.52436/1.jutif.6.4.4880

thereby supporting improved model accuracy. The Pearson correlation coefficient used in this method is calculated as (1).

$$r = \frac{\sum(x_i-\bar{x})(y_i-\bar{y})}{\sqrt{\sum(x_i-\bar{x})^2\sum(y_i-\bar{y})^2}} \quad (1)$$

In this context, r represents the Pearson correlation coefficient, which quantifies the strength and direction of the linear relationship between the input feature and the target class. x_i\ represents the value of the input feature, y_i\ denotes the corresponding class label, while\ \bar{x} and \bar{y} refer to the mean of the feature and the mean of the target class, respectively. The aforemention expression is applied into three agricultural datasets to evaluate the correlation between individual target class and features, as well as to examine the relationships among the features themselves. The results of this analysis are presented in Figure 3.

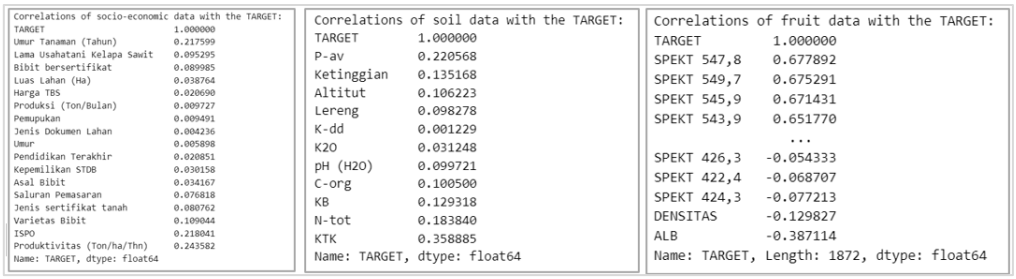

Figure 3. Correlation with Target Result of Agricultural Datasets

After calculating the correlation coefficients for the features, a thresholding process was applied to determine the most informative variables for each set of agricultural data. Specifically, features with correlation values exceeding thresholds of 0.2 for socio-economic data, 0.2 for soil data, and 0.65 for fruit data were retained as the most significant contributors to the target class. These selected features were then used as inputs for feature extraction within the Convolutional Neural Network (CNN). By focusing on these optimized feature subsets, the CNN is able to process a more refined dataset, enhancing its learning capability and generalization performance. This step is essential for building a robust predictive model that leverages the strongest predictors identified in the data. The results of the feature selection are illustrated in Figure 4 and including the selected agricultural features used for integration with thermal images are detailed in Table 2.

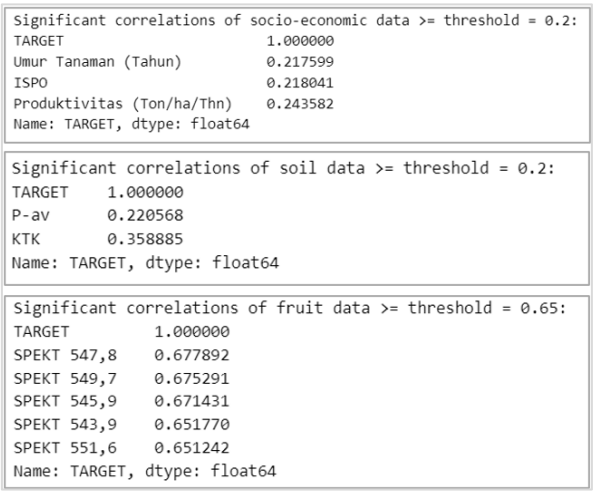

Figure 4. Selected Features of Agricultural Datasets

Vol. 6, No. 4, Agustus 2025, Page. 2035-2052
https://jutif.if.unsoed.ac.id
DOI: https://doi.org/10.52436/1.jutif.6.4.4880

Figure 4 visualizes the correlation scores of individual features from the three agricultural datasets with respect to the target class. The result highlights which variables surpassed the defined thresholds and were consequently selected for integration. This figure serves to illustrate the effectiveness of the correlation-based feature selection process and the relative importance of each variable category (socio-economic, soil, and spectral fruit).

Table 2. Agricultural Data Features Used for Multimodal Integration

Agricultural Data	Features to be Combined with the Image
Socio-economic	Umur Tanaman (Tahun), Produktivitas(Ton/ha/Thn), ISPO
Soil	P-av, KTK
Spectral Fruit	SPEKT 547,8, SPEKT 549,7, SPEKT 545,9, SPEKT 543,9, SPEKT 551,6

Table 2 lists the specific agricultural features that were retained after thresholding and subsequently integrated with thermal image data. It includes the feature names and their data source (e.g., soil, socio-economic, or spectral fruit). This table provides a clear overview of which features were deemed most relevant and helps justify their inclusion in the multimodal deep learning model.

2.2.3. Normalization, Resizing, and Feature Preparation

In this study, a comprehensive preprocessing pipeline was implemented to prepare both thermal images and supporting agricultural data for model training. Thermal images were resized to a consistent resolution of 96×96 pixels to maintain uniformity and compatibility with the input layer of the CNN architectures. Values of the pixels in the images were normalized by scaling them to the range [0, 1] through division by 255, which facilitates faster convergence during training [32].

Concurrently, agricultural data from socio-economic, soil, and spectral fruit datasets were aggregated and aligned based on their class labels. The features from these diverse sources were merged into a unified dictionary, ensuring consistent key formatting by converting all class labels to uppercase and removing whitespace. For each class, the combined feature vectors were constructed by extracting values corresponding to a consolidated set of all relevant feature keys, filling missing entries with zeros to maintain dimensional consistency. The results of this aggregation and alignment process are illustrated in Figure 5, which shows a sample of the unified feature vectors. These combined agricultural feature vectors are subsequently integrated with thermal image inputs within the classification framework, enabling the model to learn from both visual and contextual data for improved accuracy.

```
Class 'ab 1' -> Normalized: 'AB1', Images Loaded: 102
Socio-economic Additional Feature:
{'Umur Tanaman (Tahun)': 5.333333333333333, 'ISPO': 3.0, 'Produktivitas (Ton/ha/Thn)': 13.333333333333334}
Soil Data Additional Feature:
{'P-av': 2.9, 'KTK': 10.4}
Fruit Data Additional Feature:
{'SPEKT 547,8': 15.1, 'SPEKT 549,7': 14.2, 'SPEKT 545,9': 16.2, 'SPEKT 543,9': 16.4, 'SPEKT 551,6': 14.0}
Class 'ab 10' -> Normalized: 'AB10', Images Loaded: 100
Socio-economic Additional Feature:
{'Umur Tanaman (Tahun)': 9.0, 'ISPO': 4.0, 'Produktivitas (Ton/ha/Thn)': 12.777777777777779}
Soil Data Additional Feature:
{'P-av': 1.3, 'KTK': 17.2}
Fruit Data Additional Feature:
{'SPEKT 547,8': 72.6, 'SPEKT 549,7': 84.3, 'SPEKT 545,9': 59.9, 'SPEKT 543,9': 50.8, 'SPEKT 551,6': 91.7}
Class 'ab 11' -> Normalized: 'AB11', Images Loaded: 102
Socio-economic Additional Feature:
{'Umur Tanaman (Tahun)': 10.666666666666666, 'ISPO': 3.3333333333333335, 'Produktivitas (Ton/ha/Thn)': 14.666666666666666}
Soil Data Additional Feature:
{'P-av': 1.3, 'KTK': 17.2}
Fruit Data Additional Feature:
{'SPEKT 547,8': 59.9, 'SPEKT 549,7': 68.8, 'SPEKT 545,9': 49.7, 'SPEKT 543,9': 45.8, 'SPEKT 551,6': 74.2}
Class 'ab 12' -> Normalized: 'AB12', Images Loaded: 101
Socio-economic Additional Feature:
...
```

Figure 5. Aggregated Agricultural Feature Vectors by Class Labels

Vol. 6, No. 4, Agustus 2025, Page. 2035-2052
https://jutif.if.unsoed.ac.id
DOI: https://doi.org/10.52436/1.jutif.6.4.4880

Additionally, categorical class labels were standardized and encoded into numerical formats using label encoding to maintain uniformity across the dataset. The aggregated feature dictionaries were then vectorized into numerical arrays compatible with the model input requirements. Feature normalization was performed utilizing StandardScaler, which normalizes each feature by subtracting the mean and adjusting to unit variance [33], [34], as shown in the equation (2).

$$X' = \frac{X-\mu}{\sigma} \quad (2)$$

The standardized value, denoted as $\boldsymbol{X'}$, is obtained by subtracting the mean μ of the feature from the original value $\boldsymbol{X}$, and then dividing the result by the standard deviation $\boldsymbol{\sigma}$ of that feature. This vectorization, combined with image resizing and normalization, effectively reshapes and aligns the multi-modal input data, facilitating seamless integration within the CNN framework. This integrated preprocessing step ensures that both image and tabular agricultural data are properly formatted, normalized, and synchronized, enabling the model to leverage heterogeneous data sources effectively for improved classification performance.

2.2.4. Split Data

To evaluate the effectiveness and resilience of the classification models, The dataset was split into three portions: 70% for training, 20% for validation, and 10% for testing. The model parameters were trained using the training set, whereas the validation set was employed to fine-tune hyperparameters and track for overfitting. The test set was reserved for the final evaluation to provide an unbiased measure of the model's generalization to unseen data. A Stratified selection was applied to ensure that the distribution of classes remained consistent across all subsets, preserving class balance and supporting reliable performance assessment [35].

2.3. CNN Models: ResNet50 and MobileNet

This study employs two widely recognized Convolutional Neural Network (CNN) architectures, ResNet50 and MobileNet, to classify the origin of palm oil seeds based on thermal images and supporting agricultural data. ResNet50 is utilized for its capability to train very deep networks effectively by leveraging residual connections that alleviate the vanishing gradient problem, enabling robust feature extraction from complex thermal images [36]. MobileNet was preferred for its efficient architecture, which leverages depthwise separable convolutions to minimize resource usage while still delivering reliable performance. Therefore, MobileNet can be effectively applied for deployment in resource-constrained environments [37].

Both models are initialized with pretrained weights from ImageNet and adapted by removing their top fully connected layers to serve as feature extractors. The extracted feature maps from the CNN backbone are then processed through a global average pooling layer which transforms spatial features into fixed-length vectors. These image feature vectors are subsequently combined with agricultural data features through a concatenation layer, followed by fully connected layers utilizing ReLU activations and dropout regularization to capture complex relationships between multimodal inputs. In the final stage, a softmax-activated output layer is used to produce class probabilities corresponding to seed origin labels.

This model design enables the integration of visual and tabular data, enabling the model to capture intricate correlations between diverse input types. The MobileNet model shares the same architecture, differing only in the choice of the CNN backbone, facilitating a fair comparison between the two CNN variants. Furthermore, this study evaluates the effectiveness performance of ResNet50 and MobileNet architectures to recognize the highest-performing model for this multimodal classification task. The overall architecture of the proposed multimodal CNN model is illustrated in Figure 6.

Vol. 6, No. 4, Agustus 2025, Page. 2035-2052
https://jutif.if.unsoed.ac.id
DOI: https://doi.org/10.52436/1.jutif.6.4.4880

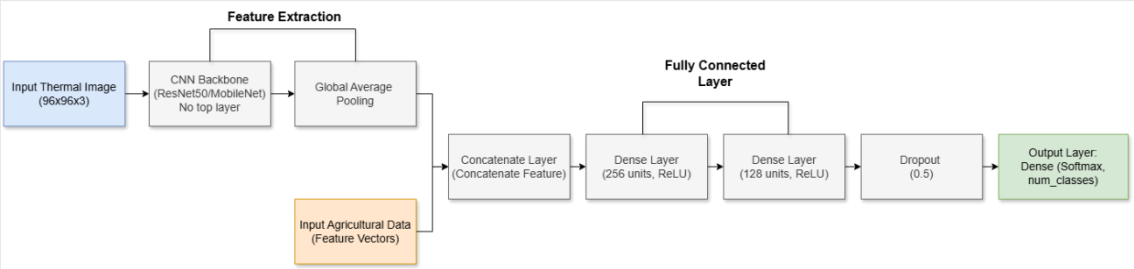

Figure 6. Proposed Multimodal CNN Architecture for Palm Seed Origin Classification

2.4. Hyperparameter Tuning

Hyperparameter optimization constitutes a fundamental aspect of deep learning model development, as it significantly affects the model's learning dynamics and its capacity to generalize effectively to previously unseen data. Proper tuning of hyperparameters such as optimizer, learning rate, and batchsize choice can significantly enhance model performance, reduce training time, and prevent issues like overfitting or underfitting. According to a study [38], optimizing machine learning model performance and generalization critically depends on effective hyperparameter tuning, which plays a vital role across a range of applications and involves diverse optimization strategies.

In this study, Hyperparameter tuning was conducted on the model demonstrating the best result from the initial comparison between ResNet50 and MobileNet architectures. The tuning process systematically explored 12 different combinations of core training settings, comprising learning rate, optimizer, and batch size, as shown in Table 3.

Table 3. Hyperparameter Settings

Hyperparameter	Value
Optimizer	Adam and SGD
Learning Rate	0.001 and 0.0001
Batchsize	16, 32, and 64

The tuning involved varying the learning rate between 0.001 and 0.0001, experimenting with batch sizes of 16, 32, and 64, and testing two popular optimizers: Adam and Stochastic Gradient Descent (SGD). Each combination was evaluated based on validation accuracy and loss with the goal of selecting the most effective parameter combination for classification performance while maintaining model generalizability.

2.5. Evaluation Metrics

To comprehensively assess the classification models performance, various evaluation metrics were employed. These metrics offer a multifaceted view of the models' predictive capabilities, capturing not only the overall correctness but also the quality of predictions in terms of precision, sensitivity, and ensuring consistent performance across both types of classification errors. Evaluating models through a variety of metrics is especially important in scenarios where class distributions are imbalanced, as relying solely on accuracy can be misleading [39]. By incorporating metrics such as, recall, precission and F1-score, the evaluation framework provides a deeper understanding of the model's strengths and limitations in correctly identifying each class, ultimately determining a robust and accurate measurement of classification performance [40].

Vol. 6, No. 4, Agustus 2025, Page. 2035-2052
https://jutif.if.unsoed.ac.id
DOI: https://doi.org/10.52436/1.jutif.6.4.4880

2.5.1. Accuracy

The accuracy metric quantifies the proportion of correctly predicted instances relative to the overall number of cases assessed, and can be computed using the following expression (3).

$$Accuracy = \left(\frac{TP+TN}{TP+TN+FP+FN}\right) \quad (3)$$

TP refers to true positives, TN is true negatives, FP refers to false positives, and FN is false negatives. Although accuracy gives an overall indication of the model's correctness, it may not be reliable when the class distribution in the dataset is skewed.

2.5.2. Precision

Precision indicates the proportion of true positive predictions among all instances that the model classified as positive, reflecting the accuracy of positive predictions. It is defined as (4).

$$Precision = \left(\frac{TP}{TP+FP}\right) \quad (4)$$

High precision indicates a low false positive rate, reflecting the model's ability to avoid misclassifying negative samples as positive.

2.5.3. Recall

Recall assesses the model capability to identify all true instances of the positive class. It is calculated as the proportion of true positives to the total actual positive cases, including true positives and false negatives. It is defined as (5).

$$Recall = \left(\frac{TP}{TP+FN}\right) \quad (5)$$

A high recall value signifies that the model is highly effective at identifying the majority of actual positive cases within the dataset. This means that the model has a strong ability to minimize false negatives, which is particularly important in scenarios where failing to detect positive instances could lead to significant consequences.

2.5.4. F1-Score

F1-Score combines precision and recall as a harmonic mean, offering a comprehensive metric that balances the two. A high F1-Score reflects strong performance in both precision and recall simultaneously. It is defined as (6).

$$F1 - Score = \frac{2 * Precision * Recall}{Precision + Recall} \quad (6)$$

3. RESULT

The following section reports the outcomes of the classification models evaluated on the palm oil seed origin task. The models were tested in three configurations: (1) using thermal images only, (2) combining thermal images with agricultural data, and (3) applying hyperparameter tuning to the best-performing model. The performance of each model was evaluated using various metrics, including accuracy, precision, recall, and F1-score. The findings highlight how the integration of multimodal data enhances classification effectiveness and reveal notable performance improvements resulting from hyperparameter tuning.

Vol. 6, No. 4, Agustus 2025, Page. 2035-2052
https://jutif.if.unsoed.ac.id
DOI: https://doi.org/10.52436/1.jutif.6.4.4880

3.1. Model on Thermal Image Only

In this configuration, both ResNet50 and MobileNet models were trained and evaluated using thermal images alone. For the experiments, the thermal images were resized to 96×96 pixels and normalized before being fed into the pretrained CNN backbones (ResNet50 and MobileNet) to extract features. After feature extraction, the features were passed through fully connected layers with ReLU activation, dropout regularization, and a softmax output layer to predict the seed origin. In this experiment, a batch size of 32 and a learning rate of 0.0001 were used during training, with the Adam optimizer selected for optimization. Model performance was evaluated by monitoring accuracy and loss throughout both the training and validation phases, while final test accuracy was recorded to assess generalization capability. The results are summarized in the Table 4.

Table 4. Performance Comparison of ResNet50 and MobileNet Using Thermal Images Only

Model	Epoch	Batch	LR	Optimizer	Train Accuracy	Train Loss	Val Accuracy	Val Loss	Test Accuracy
ResNet50	**30**	**32**	**0.0001**	**Adam**	**99.64%**	**0.0175**	**67.79%**	**1.9205**	**69.42%**
MobileNet	30	32	0.0001	Adam	98.20%	0.0874	64.80%	1.5887	63.22%

As shown in Table 4, ResNet50 outperformed MobileNet in this configuration, likely due to its deeper architecture and superior ability to capture more complex features from the thermal images. In the thermal image-only setup, ResNet50 achieved a test accuracy of 69.42%, while MobileNet reached 63.22%, indicating a clear performance gap. This suggests that ResNet50 is more effective in learning discriminative features from thermal input alone, making it a more suitable choice when using visual data without additional contextual information, as reflected by its precision of 73.26%, recall of 69.42%, and F1-score of 69.98%. The results confirm that model depth and representational power play an important role in achieving better classification performance when relying solely on image-based inputs.

3.2. Model on Thermal Image and Agricultural Data

In the next configuration, the models were extended by incorporating agricultural data alongside thermal images. The agricultural data, which consists of socio-economic, soil, and spectral fruit features, was provided as a separate input vector. These features were concatenated with the features extracted from the thermal images using the Concatenate layer. Thermal images were resized to 96×96 pixels and normalized before being fed into the pretrained CNN backbones (ResNet50 and MobileNet). The CNN architectures served to extract feature representations from the thermal images, which were then passed through a global average pooling layer to produce fixed-length feature vectors.

The concatenation of these two distinct feature sets, thermal image features and agricultural data features, was done by the Concatenate layer in Keras, which combines the output from both sources into a single feature vector. This combined feature vector, containing both visual and tabular data, was subsequently processed through a series of fully connected layers utilizing ReLU activation and dropout for regularization, followed by a softmax output layer to perform seed origin classification.

The models were optimized using a batch size of 32, a learning rate of 0.0001, and the Adam optimizer. Their performance was systematically evaluated based on metrics including training accuracy and loss, validation accuracy and loss, as well as final test accuracy. The results are summarized in the Table 5.

Vol. 6, No. 4, Agustus 2025, Page. 2035-2052
https://jutif.if.unsoed.ac.id
DOI: https://doi.org/10.52436/1.jutif.6.4.4880

Table 5. Performance Comparison of ResNet50 and MobileNet Using Thermal Images Combined with Agricultural Data

Model	Epoch	Batch	LR	Optimizer	Train Accuracy	Train Loss	Val Accuracy	Val Loss	Test Accuracy
ResNet50	**30**	**32**	**0.0001**	**Adam**	**99.64%**	**0.0258**	**68.71%**	**1.6537**	**71.07%**
MobileNet	30	32	0.0001	Adam	98.49%	0.0718	71.00%	1.2699	69.70%

As shown in Table 5, the integration of agricultural data resulted in performance improvements across both models, with ResNet50 achieving the highest test accuracy of 71.07%, along with an overall precision of 73.15%, recall of 71.07%, and F1-score of 71.04%. Compared to the thermal image-only configuration, this multimodal approach led to a clear performance gain, highlighting the significant contribution of agricultural features such as socio-economic, soil, and spectral fruit data. These features provided additional context that enriched the information extracted from thermal images, enabling the model to distinguish class characteristics more effectively. The results demonstrate that integrating agricultural data with visual inputs not only enhances classification accuracy but also improves model robustness and generalization.

3.3. Hyperparameter Tuning on Best Model

Hyperparameter tuning was applied to ResNet50, the model that demonstrated superior performance in both thermal image-only and multimodal configurations. A total of 12 training combinations were evaluated by varying batch sizes (16, 32, 64), learning rates (0.001 and 0.0001), and optimizers (Adam and SGD) to identify the most effective configuration. The tuning results showed that the Adam optimizer facilitated faster convergence within 20 to 30 epochs, while SGD required extended training ranging from 70 to 100 epochs to achieve comparable results. Moreover, the learning rate had a critical influence on training duration and model accuracy. Higher learning rates typically accelerated convergence, whereas lower learning rates enabled more gradual refinement, particularly when using SGD.

Table 6. Summary of Best Hyperparameter Tuning Results for ResNet50

Number	Epoch	Batch	LR	Optimizer	Train Accuracy	Train Loss	Val Accuracy	Val Loss	Test Accuracy
1	**20**	**16**	**0.001**	**Adam**	**99.75%**	**0.0126**	**99.92%**	**0.0014**	**100.00%**
2	30	16	0.0001	Adam	99.35%	0.0286	71.92%	1.5407	73.42%
3	70	16	0.001	SGD	99.67%	0.0184	80.72%	0.8670	80.30%
4	100	16	0.0001	SGD	97.59%	0.1318	65.88%	1.5598	65.70%
5	20	32	0.001	Adam	99.22%	0.0359	99.46%	0.0207	99.17%
6	30	32	0.0001	Adam	99.71%	0.0155	70.85%	1.6405	70.11%
7	70	32	0.001	SGD	99.10%	0.0488	69.70%	1.4949	69.70%
8	100	32	0.0001	SGD	96.75%	0.1785	57.23%	1.8215	54.82%
9	20	64	0.001	Adam	99.10%	0.0386	93.11%	0.2645	92.01%
10	30	64	0.0001	Adam	99.50%	0.0244	68.94%	1.8865	61.43%
11	70	64	0.001	SGD	99.43%	0.0364	64.42%	1.7772	62.53%
12	100	64	0.0001	SGD	97.74%	0.1506	51.42%	2.0675	52.20%

Vol. 6, No. 4, Agustus 2025, Page. 2035-2052
https://jutif.if.unsoed.ac.id
DOI: https://doi.org/10.52436/1.jutif.6.4.4880

However, configurations involving excessively long training durations or poorly tuned learning rates introduced the risk of model instability. When the learning rate is too high, the model may exhibit oscillating behavior due to overly aggressive weight updates, preventing it from converging to an optimal solution. On the other hand, very small learning rates may cause slow learning and increase the risk of overfitting during prolonged training. Therefore, selecting appropriate hyperparameter values is crucial to ensure model stability, effective convergence, and improved generalization performance. Table 6 summarizes the results from the 12 combinations tested during the tuning process.

As shown in Table 6, the best-performing model achieved outstanding results with a training accuracy of 99.75%, validation accuracy of 99.92%, and a perfect test accuracy of 100% using the Adam optimizer with a learning rate of 0.001 and a batch size of 16. This combination allowed the model to converge quickly, with 20 epochs providing optimal training. In contrast, the SGD optimizer, despite requiring more epochs (70-100), did not outperform Adam in terms of test accuracy. These results emphasize the importance of hyperparameter tuning, where the Adam optimizer with a learning rate of 0.001 and batch size of 16 proved to be the most effective configuration for palm oil seed origin classification. The classification performance metrics of the ResNet50 model with optimal hyperparameters are shown in Figure 7, providing a detailed breakdown of evaluation scores including accuracy, precision, recall, and F1-score.

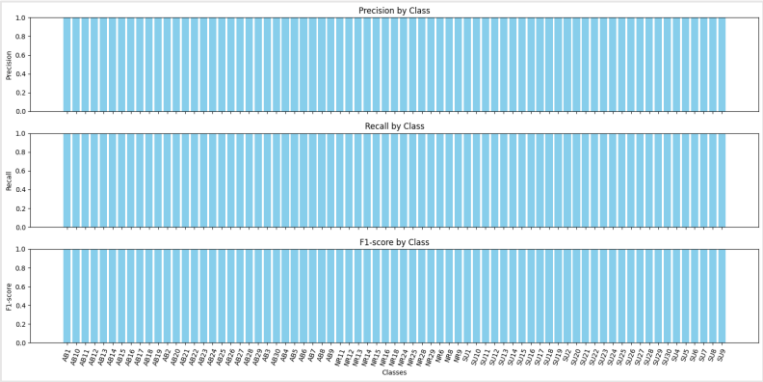

Figure 7. Classification Performance Metrics for ResNet50 with Optimal Hyperparameters

Evaluation metrics such as precision, recall, F1-score, and accuracy were employed to further confirm the robustness of the most effective model. As shown in Figure 7, the model achieved perfect scores across all metrics, with 100.00% for precision, recall, F1-score, and overall accuracy. These results confirm that the model not only performed well on the training and validation sets but also generalized exceptionally on the test set, accurately classifying all classes without error. This consistent and flawless performance highlights the effectiveness of the proposed architecture and the selected hyperparameter configuration in classifying palm oil seed origins with high reliability.

3.4. Comparative Performance Summary

To provide a clearer overview of model performance across different configurations, a comparative summary is presented in Table 7.

As shown in Table 7, a comparative summary of model performance is presented to illustrate the effectiveness of different configurations. The table includes training, validation, and test accuracies for three experimental setups: using thermal images only, using multimodal input (thermal + agricultural data), and applying hyperparameter tuning to the best-performing model (ResNet50). This comparison clearly demonstrates that incorporating agricultural data alongside thermal imagery significantly improves model performance. Moreover, applying hyperparameter tuning further enhances the model's learning ability and generalization, achieving a perfect test accuracy of 100% in the best configuration.

Vol. 6, No. 4, Agustus 2025, Page. 2035-2052
https://jutif.if.unsoed.ac.id
DOI: https://doi.org/10.52436/1.jutif.6.4.4880

Table 7. Performance Comparison of Resnet50 Model Configurations

Configuration	Epoch	Batch	LR	Optimizer	Train Accuracy	Train Loss	Val Accuracy	Val Loss	Test Accuracy
Thermal Only	30	32	0.0001	Adam	99.64%	0.0175	67.79%	1.9205	69.42%
Multimodal	30	32	0.0001	Adam	99.64%	0.0258	68.71%	1.6537	71.07%
Multimodal + Tuning	20	16	0.001	Adam	99.75%	0.0126	99.92%	0.0014	100.00%

4. DISCUSSIONS

In this study, integrating thermal images with agricultural data resulted in significant improvements in model classification performance. The ResNet50 model outperformed MobileNet in both configurations, including thermal image only and thermal image combined with agricultural data. This superiority is likely due to its deeper architecture, which allowed it to extract and learn more complex visual features. In contrast, MobileNet performed well in scenarios with limited computational resources, demonstrating its efficiency for deployment in lightweight environments despite its relatively lower accuracy. Similar findings were reported in prior work [23], where deeper CNNs like ResNet were found to be more effective for fine-grained agricultural classification tasks.

The combination of thermal image features with supporting agricultural data, which included socio-economic, soil, and spectral fruit variables, delivered enriching data that boosted the model's ability to make accurate classifications. This multimodal approach led to better generalization, especially in real-world scenarios where both image and tabular data are available and relevant to the classification task. Previous studies [25], have also demonstrated that fusing image data with structured data can significantly improve classification accuracy in plant disease detection and other agricultural applications.

Hyperparameter tuning played a vital role in optimizing model performance. The configuration using the Adam optimizer with a learning rate of 0.001 and batch size of 16 achieved the best result. Compared to SGD, which required more epochs, Adam enabled faster and more stable convergence, highlighting the critical role of choosing suitable hyperparameters that align with the characteristics of the model and dataset. This finding is consistent with the results reported to a study [41], which demonstrated that the Adam optimizer produced better accuracy and convergence efficiency than SGD in training convolutional neural networks for image classification tasks. In addition, variations in the learning rate and number of epochs show a significant influence on the final accuracy, especially when agricultural features are added to the training process.

Figure 8 shows the best accuracy and loss plots generated in this study for the ResNet50 model over 20 epochs using the optimal hyperparameter configuration. The accuracy graph illustrates a consistent upward trend during the early epochs, followed by a stable plateau that indicates the model's ability to learn effectively from the training data while maintaining steady performance on the validation set. In parallel, the loss graph displays a continuous decrease for both training and validation, reflecting a reduction in prediction error over time. The absence of significant fluctuations as observed in the accuracy and loss curves, indicating that the model achieved strong convergence without signs of overfitting. These patterns demonstrate that the model was able to generalize well and maintain reliable performance throughout the training process.

Futhermore to optimal hyperparameter settings, the use of dropout regularization in the model architecture also contributed to its ability to avoid overfitting. Dropout works by temporarily disabling

Vol. 6, No. 4, Agustus 2025, Page. 2035-2052
https://jutif.if.unsoed.ac.id
DOI: https://doi.org/10.52436/1.jutif.6.4.4880

a subset of neurons during the training process, which helps reduce over-reliance on certain features and promotes the development of more generalized and resilient feature representations. In this study, a dropout rate of 0.5 was applied after the fully connected layers, which helped maintain a balance between model complexity and generalization. This mechanism likely played a key role in maintaining training stability and ensuring that the model performed consistently well on both the training and validation data. The effectiveness of dropout for reducing overfitting in image classification tasks has also been demonstrated in recent study [42], which confirms that dropout regularization significantly improves generalization in deep learning models by preventing the model from over-relying on specific features during training.

Although this study has shown promising results, there are several limitations that should be considered. One of the main challenges is the relatively small size of the dataset, which may limit the model's ability to perform consistently when applied to new and more diverse data. Additionally, all thermal images and agricultural may not fully represent the variability encountered in real-world environments such as different climates, sensor devices, or geographical regions. The agricultural features used in this study were also limited to a predefined set. Incorporating other relevant variables such as weather conditions, planting schedules, or historical soil data could help the model learn more contextual information and improve its classification accuracy. Furthermore, this study focused only on two convolutional neural network architectures, ResNet50 and MobileNet, from which ResNet50 was identified as the best-performing model based on its superior accuracy and generalization capability. Future research may consider exploring more advanced or efficient architectures to further improve classification accuracy and model robustness.

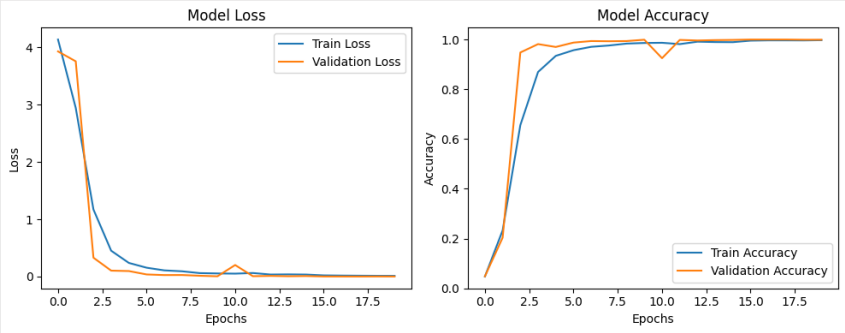

Figure 8. Train and Validation Accuracy and Loss Plot on Best Hyperparameter Tuning Model

5. CONCLUSION

This study demonstrated that the integration of thermal images with agricultural data can significantly improve the accuracy of classifying the origin of palm oil seeds. By comparing two convolutional neural network architectures, ResNet50 and MobileNet, the results showed that ResNet50 consistently outperformed MobileNet in both image-only and multimodal configurations. The use of multimodal input, combining thermal imagery with socio-economic, soil, and spectral fruit features, enabled the models to capture more comprehensive patterns, leading to better generalization across classes.

Hyperparameter tuning further enhanced model performance, with the best results achieved using the ResNet50 model configured with the Adam optimizer, a learning rate of 0.001, and a batch size of 16. This configuration produced the highest training accuracy of 99.75%, validation accuracy of 99.92%, and a perfect test accuracy of 100.00%, along with strong evaluation results including precision, recall, and F1-score of 100.00%, indicating highly reliable classification performance. The training

Vol. 6, No. 4, Agustus 2025, Page. 2035-2052
https://jutif.if.unsoed.ac.id
DOI: https://doi.org/10.52436/1.jutif.6.4.4880

process also showed fast convergence and stable validation behavior, as visualized in the accuracy and loss plots.

Overall, this research highlights the effectiveness of combining image-based and structured data in deep learning classification tasks, particularly in the context of palm oil agriculture. Future work may focus on expanding the dataset, incorporating more diverse environmental variables, and exploring newer or more efficient model architectures to improve scalability and generalizability in real-world applications.

CONFLICT OF INTEREST

The authors affirm that there are no conflicts of interest associated with the publication of this paper. All contributors have played an equal role in conducting the research and preparing the manuscript.

ACKNOWLEDGEMENT

The author would like to express gratitude to the Research Center for Rural Development and Sustainable Agriculture at Syiah Kuala University for their invaluable support in providing data for this research.

REFERENCES

[1] F. Baa Adade, "Oil Palm (Elaeis guineensis) Cultivation and Food Security in the Tropical World," in *Elaeis guineensis*, H. Kamyab, Ed., Rijeka: IntechOpen, 2022, pp. 1–5. doi: 10.5772/intechopen.98486.

[2] Badan Pusat Statistik, "Statistik Kelapa Sawit Indonesia 2023," Badan Pusat Statistik. Accessed: Jan. 17, 2025. [Online]. Available: https://www.bps.go.id/id/publication/2024/11/29/d5dcb42ab730df1be4339c34/statistik-kelapa-sawit-indonesia-2023.html

[3] N. L. Rozali *et al.*, "Omics Technologies: A Strategy to Expedite the Geographical Traceability and Authenticity of Palm Oil," *Food Bioproc Tech*, vol. 18, no. 5, pp. 4101–4128, May 2025, doi: 10.1007/s11947-024-03673-w.

[4] U. S. Ramli *et al.*, "Sustainable Palm Oil—The Role of Screening and Advanced Analytical Techniques for Geographical Traceability and Authenticity Verification," *Molecules*, vol. 25, no. 12, p. 2927, Jun. 2020, doi: 10.3390/molecules25122927.

[5] L. Cheng-Li Ooi *et al.*, "Improving oil palm sustainability with molecular-precision agriculture: yield impact of SHELL DNA testing in the Malaysian oil palm supply chain," *Sci Hortic*, vol. 321, p. 112305, Nov. 2023, doi: 10.1016/j.scienta.2023.112305.

[6] X. Li, J. Du, W. Li, and F. Shahzad, "Green ambitions: A comprehensive model for enhanced traceability in agricultural product supply chain to ensure quality and safety," *J Clean Prod*, vol. 420, p. 138397, Sep. 2023, doi: 10.1016/j.jclepro.2023.138397.

[7] D. Shao and N. Marwa, "Blockchain-enabled smart contracts for enhancing seed certification transparency: A design science approach," *Smart Agricultural Technology*, vol. 9, p. 100651, Dec. 2024, doi: 10.1016/j.atech.2024.100651.

[8] H. R. Hasan *et al.*, "Smart agriculture assurance: IoT and blockchain for trusted sustainable produce," *Comput Electron Agric*, vol. 224, p. 109184, Sep. 2024, doi: 10.1016/j.compag.2024.109184.

[9] A. Y. Khaled, C. A. Parrish, and A. Adedeji, "Emerging nondestructive approaches for meat quality and safety evaluation—A review," *Compr Rev Food Sci Food Saf*, vol. 20, no. 4, pp. 3438–3463, Jul. 2021, doi: 10.1111/1541-4337.12781.

[10] Y. Gao, H. Wang, M. Li, and W.-H. Su, "Automatic Tandem Dual BlendMask Networks for Severity Assessment of Wheat Fusarium Head Blight," *Agriculture*, vol. 12, no. 9, p. 1493, Sep. 2022, doi: 10.3390/agriculture12091493.

Vol. 6, No. 4, Agustus 2025, Page. 2035-2052
https://jutif.if.unsoed.ac.id
DOI: https://doi.org/10.52436/1.jutif.6.4.4880

[11] G. Choudhary and D. Sethi, "From Conventional Approach to Machine Learning and Deep Learning Approach: An Experimental and Comprehensive Review of Image Fusion Techniques," *Archives of Computational Methods in Engineering*, vol. 30, no. 2, pp. 1267–1304, Mar. 2023, doi: 10.1007/s11831-022-09833-5.

[12] J. A. Wani, S. Sharma, M. Muzamil, S. Ahmed, S. Sharma, and S. Singh, "Machine Learning and Deep Learning Based Computational Techniques in Automatic Agricultural Diseases Detection: Methodologies, Applications, and Challenges," *Archives of Computational Methods in Engineering*, vol. 29, no. 1, pp. 641–677, Jan. 2022, doi: 10.1007/s11831-021-09588-5.

[13] Z. H. Arif *et al.*, "Comprehensive Review of Machine Learning (ML) in Image Defogging: Taxonomy of Concepts, Scenes, Feature Extraction, and Classification techniques," *IET Image Process*, vol. 16, no. 2, pp. 289–310, Feb. 2022, doi: 10.1049/ipr2.12365.

[14] S. Zolfagharnassab, A. R. B. M. Shariff, R. Ehsani, H. Z. Jaafar, and I. Bin Aris, "Classification of Oil Palm Fresh Fruit Bunches Based on Their Maturity Using Thermal Imaging Technique," *Agriculture*, vol. 12, no. 11, p. 1779, Oct. 2022, doi: 10.3390/agriculture12111779.

[15] R. Adhitama Putra Hernanda, H. Lee, J. Cho, G. Kim, B.-K. Cho, and M. S. Kim, "Current trends in the use of thermal imagery in assessing plant stresses: A review," *Comput Electron Agric*, vol. 224, p. 109227, Sep. 2024, doi: 10.1016/j.compag.2024.109227.

[16] T. Wen, J.-H. Li, Q. Wang, Y.-Y. Gao, G.-F. Hao, and B.-A. Song, "Thermal imaging: The digital eye facilitates high-throughput phenotyping traits of plant growth and stress responses," *Science of The Total Environment*, vol. 899, p. 165626, Nov. 2023, doi: 10.1016/j.scitotenv.2023.165626.

[17] S. E. Widodo, S. Waluyo, Zulferiyenni, and R. Latansya, "Detection of fruit maturity of 'Cavendish' banana using thermal image processing," 2023, p. 050003. doi: 10.1063/5.0135795.

[18] R. R. Patil and S. Kumar, "Rice-Fusion: A Multimodality Data Fusion Framework for Rice Disease Diagnosis," *IEEE Access*, vol. 10, pp. 5207–5222, 2022, doi: 10.1109/ACCESS.2022.3140815.

[19] P. Nagpal, S. A. Bhinge, and A. Shitole, "A Comparative Analysis of ResNet Architectures," in *2022 International Conference on Smart Generation Computing, Communication and Networking (SMART GENCON)*, IEEE, Dec. 2022, pp. 1–8. doi: 10.1109/SMARTGENCON56628.2022.10083966.

[20] L. Borawar and R. Kaur, "ResNet: Solving Vanishing Gradient in Deep Networks," 2023, pp. 235–247. doi: 10.1007/978-981-19-8825-7_21.

[21] B. Li, "Lightweight Neural Networks," in *Embedded Artificial Intelligence*, Singapore: Springer Nature Singapore, 2024, pp. 43–74. doi: 10.1007/978-981-97-5038-2_3.

[22] S.-F. Hsiao and B.-C. Tsai, "Efficient Computation of Depthwise Separable Convolution in MoblieNet Deep Neural Network Models," in *2021 IEEE International Conference on Consumer Electronics-Taiwan (ICCE-TW)*, IEEE, Sep. 2021, pp. 1–2. doi: 10.1109/ICCE-TW52618.2021.9602973.

[23] E. Prasiwiningrum and A. Lubis, "Classification Of Palm Oil Maturity Using CNN (Convolution Neural Network) Modelling RestNet 50," *Decode*, vol. 4, no. 3, pp. 983–999, 2024, doi: 10.51454/decode.v4i3.822.

[24] Venkatesh, N. Y, S. U. Hegde, and S. S, "Fine-tuned MobileNet Classifier for Classification of Strawberry and Cherry Fruit Types," in *2021 International Conference on Computer Communication and Informatics (ICCCI)*, IEEE, Jan. 2021, pp. 1–8. doi: 10.1109/ICCCI50826.2021.9402444.

[25] M. S. A. M. Al-gaashani, F. Shang, M. S. A. Muthanna, M. Khayyat, and A. A. Abd El-Latif, "Tomato leaf disease classification by exploiting transfer learning and feature concatenation," *IET Image Process*, vol. 16, no. 3, pp. 913–925, Feb. 2022, doi: 10.1049/ipr2.12397.

[26] M. Bilal, G. Ali, M. W. Iqbal, M. Anwar, M. S. A. Malik, and R. A. Kadir, "Auto-Prep: Efficient and Automated Data Preprocessing Pipeline," *IEEE Access*, vol. 10, pp. 107764–107784, 2022, doi: 10.1109/ACCESS.2022.3198662.

[27] K. Rahul, R. K. Banyal, and N. Arora, "A systematic review on big data applications and scope for industrial processing and healthcare sectors," *J Big Data*, vol. 10, no. 1, p. 133, Aug. 2023, doi: 10.1186/s40537-023-00808-2.

Vol. 6, No. 4, Agustus 2025, Page. 2035-2052
https://jutif.if.unsoed.ac.id
DOI: https://doi.org/10.52436/1.jutif.6.4.4880

[28] K. Maharana, S. Mondal, and B. Nemade, "A review: Data pre-processing and data augmentation techniques," *Global Transitions Proceedings*, vol. 3, no. 1, pp. 91–99, Jun. 2022, doi: 10.1016/j.gltp.2022.04.020.

[29] C. Li, X. Ren, and G. Zhao, "Machine-Learning-Based Imputation Method for Filling Missing Values in Ground Meteorological Observation Data," *Algorithms*, vol. 16, no. 9, p. 422, Sep. 2023, doi: 10.3390/a16090422.

[30] L. Wang, S. Jiang, and S. Jiang, "A feature selection method via analysis of relevance, redundancy, and interaction," *Expert Syst Appl*, vol. 183, p. 115365, Nov. 2021, doi: 10.1016/j.eswa.2021.115365.

[31] D. Effrosynidis and A. Arampatzis, "An evaluation of feature selection methods for environmental data," *Ecol Inform*, vol. 61, p. 101224, Mar. 2021, doi: 10.1016/j.ecoinf.2021.101224.

[32] H. A. Alenizy and J. Berri, "Transforming tabular data into images via enhanced spatial relationships for CNN processing," *Sci Rep*, vol. 15, no. 1, p. 17004, May 2025, doi: 10.1038/s41598-025-01568-0.

[33] L. Wossnig, N. Furtmann, A. Buchanan, S. Kumar, and V. Greiff, "Best practices for machine learning in antibody discovery and development," *Drug Discov Today*, vol. 29, no. 7, p. 104025, Jul. 2024, doi: 10.1016/j.drudis.2024.104025.

[34] M. Mokoatle, V. Marivate, D. Mapiye, R. Bornman, and Vanessa. M. Hayes, "A review and comparative study of cancer detection using machine learning: SBERT and SimCSE application," *BMC Bioinformatics*, vol. 24, no. 1, p. 112, Mar. 2023, doi: 10.1186/s12859-023-05235-x.

[35] M. Carvalho, A. J. Pinho, and S. Brás, "Resampling approaches to handle class imbalance: a review from a data perspective," *J Big Data*, vol. 12, no. 1, p. 71, Mar. 2025, doi: 10.1186/s40537-025-01119-4.

[36] D. Mohnish Kumaar and S. Palani, "ResNet50 Integrated Vision Transformer for Enhanced Plant Disease Classification," in *2024 3rd International Conference on Artificial Intelligence For Internet of Things (AIIoT)*, IEEE, May 2024, pp. 1–6. doi: 10.1109/AIIoT58432.2024.10574771.

[37] H. Yuan, J. Cheng, Y. Wu, and Z. Zeng, "Low-res MobileNet: An efficient lightweight network for low-resolution image classification in resource-constrained scenarios," *Multimed Tools Appl*, vol. 81, no. 27, pp. 38513–38530, Nov. 2022, doi: 10.1007/s11042-022-13157-8.

[38] J. A Ilemobayo *et al.*, "Hyperparameter Tuning in Machine Learning: A Comprehensive Review," *Journal of Engineering Research and Reports*, vol. 26, no. 6, pp. 388–395, Jun. 2024, doi: 10.9734/jerr/2024/v26i61188.

[39] H. Kaur, H. S. Pannu, and A. K. Malhi, "A Systematic Review on Imbalanced Data Challenges in Machine Learning," *ACM Comput Surv*, vol. 52, no. 4, pp. 1–36, Jul. 2020, doi: 10.1145/3343440.

[40] Ž. Đ. Vujovic, "Classification Model Evaluation Metrics," *International Journal of Advanced Computer Science and Applications*, vol. 12, no. 6, 2021, doi: 10.14569/IJACSA.2021.0120670.

[41] J. Zulkarnain, Kusrini, and T. Hidayat, "Klasifikasi Tingkat Kematangan Tandan Buah Segar Kelapa Sawit Menggunakan Pendekatan Deep Learning," *JST (Jurnal Sains dan Teknologi)*, vol. 12, no. 3, Jan. 2024, doi: 10.23887/jstundiksha.v12i3.59140.

[42] H. P. Kiki Iranda, A. Candra, and A. Harjoko, "Dropout regularization to overcome the overfitting of the ResNet-50 CNN algorithm in oil palm leaf disease classification," 2024, p. 020006. doi: 10.1063/5.0207210.

Jurnal Teknik Informatika (JUTIF)
P-ISSN: 2723-3863
E-ISSN: 2723-3871
Vol. 6, No. 4, Agustus 2025, Page. 2035-2052
https://jutif.if.unsoed.ac.id
DOI: https://doi.org/10.52436/1.jutif.6.4.4880